Infrared Physics & Technology 122 (2022) 104080

Contents lists available at ScienceDirect

Infrared Physics and Technology

journal homepage: www.elsevier.com/locate/infrared

10.6 μm saturable absorption and optical isolation of graphene

Ranran Zhang [a], Qikun Pan [a,*], Fei Xu [a,b], Jin Guo [a], Fei Chen [a], Deyang Yu [a], Junjie Sun [a], Kuo Zhang [a], Yang He [a], Yi Chen [a]

[a] State Key Laboratory of Laser Interaction with Matter, Changchun Institute of Optics, Fine Mechanics and Physics, Chinese Academy of Sciences, Changchun 130033, China
[b] University of Chinese Academy of Sciences, Beijing 100049, China

ARTICLE INFO

Keywords:
LPP-EUV
Graphene
Saturable absorption
Optical isolation

ABSTRACT

In this paper, the nonlinear absorption and optical isolation properties of graphene on a ZnSe substrate were studied at 10.6 μm. The relationships between graphene saturable absorption parameters, the damage threshold and number of layers were studied by experiment. The results show that single-layer graphene on a ZnSe substrate has a higher damage threshold and lower nonsaturable loss coefficient than multilayer graphene and is more suitable for high-power MOPA-CO_2 laser systems. The simulation results show that 90% of the small-signal noise light can be suppressed by 50 passes through single-layer graphene, and the ratio of the noise to the main pulse can be reduced from 1% to 0.15%.

1. Introduction

Nanosecond-pulse CO_2 lasers based on Master Oscillator Power-Amplifier (MOPA) plays an important role in extreme ultraviolet (EUV) lithography and other areas. The common methods of noise suppression in MOPA systems include Faraday isolation, electro-optical isolation, saturable absorption isolation, etc. [1–3]. At 10.6 μm, the most commonly used isolation method is the SF_6 saturable absorber. However, they do not fare well in high-repetition-rate applications due to a fundamental limitation of the molecular kinetics, requiring a high velocity gas circulation system to replace the bleached absorber [3].

As a saturable absorber, graphene has the advantages of a wide absorption spectrum and short relaxation time in the bleached state [4–6], and graphene has been used in the high − rep − rate lasers passive mode locking fields [7–10]. Graphene has great potential as a passive optical isolator for high-repetition-rate applications. However, to our knowledge, there are few reports on the saturable absorption characteristics at 10.6 μm and isolation ability of graphene. We first proposed the concept of graphene as an optical isolator. In this paper, the saturable absorption properties of graphene versus the number of layers at a wavelength of 10.6 μm were measured, and the feasibility of using graphene as an optical isolator was studied.

The saturable absorption parameters α_s, α_{ns}, and I_s determine the isolation performance of a passive optical isolator. The formula used to describe the saturable absorption of graphene is $\alpha(I) = \alpha_s/(1 + I/I_s) + \alpha_{ns}$, where α_s is the initial absorption coefficient, α_{ns} is the nonsaturable loss coefficient due to interlayer scattering and defects in the crystal structure [11,12], and I_s is the saturation parameter. In this paper, the transmission curves of films containing 1, 4, and 8 graphene layers were measured at 10.6 μm. In addition, the damage mechanism was clarified by the study of transmittance and surface damage. The relationships between saturable absorption parameters, the damage threshold and graphene layers were established.

After obtaining the saturation parameters and damage threshold, we simulated and evaluated the performance of graphene isolators. For passive saturable absorption isolators, the following properties are very important: high transmittance of the main laser pulse, low transmittance of small-signal intensity noise, fast relaxation of the upper level and pulse waveform evolution. Because the relaxation time of the graphene upper level is on the order of picoseconds, this paper mainly simulated the main pulse transmittance, small signal noise transmittance and pulse waveform evolution characteristics of nanosecond pulses through a multi-pass graphene optical isolator. Graphene isolators can be used in the seed light or preamplifier stage on a CO_2 laser with a MOPA system, which is a promising isolation method.

2. Measurement method

As shown in Fig. 1(a) and Fig. 1(b), to measure the transmittance of multilayer graphene films, an experimental platform based on an

* Corresponding author.
E-mail address: panqikun2005@163.com (Q. Pan).

https://doi.org/10.1016/j.infrared.2022.104080
Received 1 November 2021; Received in revised form 11 February 2022; Accepted 12 February 2022
Available online 16 February 2022

electro-optically cavity-dumped CO_2 laser was built. The repetition rate of the laser was continuously adjustable from 100 Hz to 100 kHz. The maximum average power at 1 kHz is approximately 0.7 W. The pulse width was approximately 15 ns. The spatial distribution of the beam was TEM_{00} mode. The graphene sample was placed on a precision displacement platform after focusing lens. By shifting the axial position of the test sample, the size of the beam spot and peak power density could be adjusted conveniently. The maximum incident peak power density after focusing was approximately 4.5 MW/cm^2 with a 1 mm diameter spot. To control the incident power on the test sample, we inserted an SF_6 cell at the focal point of the beam expanding system. The power adjustment range was 0%−95% by continuously changing the SF_6 pressure. The input and output power were measured by the power meter, and the transmittance was calculated by $T = I_{in}/I_{out}$.

Graphene was prepared by the CVD method and transferred to a ZnSe surface by the wet method. The number of transfer layers was controlled accurately. Therefore, the relationship between the saturable parameters and number of layers was studied. Photos of graphene and the ZnSe substrate are shown in Fig. 1(b). The evaluation of the number of damaged layers of graphene depends on transmission measurements and observations of microscopic morphology.

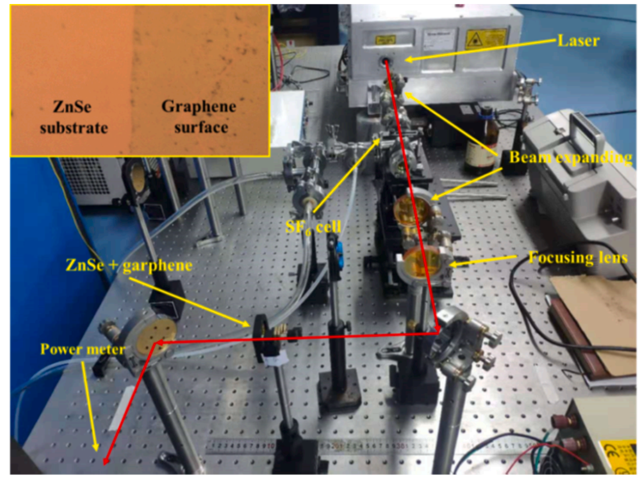

Fig. 1b. Picture of the experimental platform.

3. Ablation threshold

We measured the transmittance of graphene films that consisted of 1, 4 and 8 layers. Fig. 2 shows the dependence of graphene transmission on the peak power density of the incident laser. The transmission point with a power density of 0 was from the formula $T = (1–0.023)^n$, where n is the number of graphene layers [13]. When the incident power density on the graphene film increased from 0, the transmission gradually increased until saturation. As the power density increased, the graphene surface began to display luminescence, and the transmittance did not increase significantly until the graphene surface film was ablated. After ablation damage, the transmittance slightly increased with increasing power density as the number of graphene layers decreased. The luminescence and ablation thresholds of films with 1, 4, 8 and 12 layers are shown in Table.1. The luminescence and ablation threshold were inversely proportional to the number of layers. The ablation threshold of graphene was higher near the substrate than at the surface. The reason is that graphene has better heat dissipation performance when it is closer to the substrate.

The relationship between the transmittance and repetition rate of incident laser is shown on the right side of Fig. 3. The experimental laser used frequency modulation to adjust the power; that is, the average power was linearly proportional to the frequency, and the single pulse energy was constant. As shown in Fig. 3, the number of layers was 8, and the incident peak power was approximately 900 and 1400 kW/cm^2. When the incident peak power density was constant, the transmittance was stable, and it was independent of the laser frequency and duration of irradiation. When the peak power density of incident light was lower than the damage threshold of graphene, the transmittance and isolation performance of the graphene isolator had long-term stability. While, if the graphene surface was ablated, the transmittance did not increase further when the power density stopped increasing, this ensured the

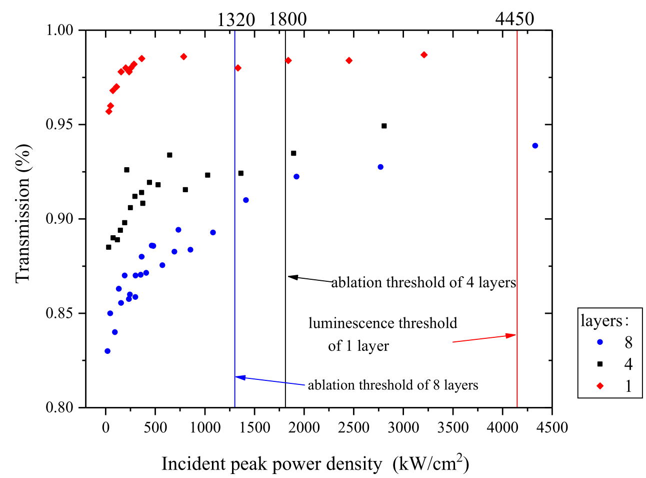

Fig. 2. Transmission measurements of graphene films.

Table 1
Luminescence and ablation thresholds of graphene films.

Number of layers	Luminescence threshold (kW/cm^2)	Ablation thresholds (kW/cm^2)
1	4450	>4450
4	1300	1800
8	1000	1320
12 (from reference [11])	700	1000

stability of graphene at 10.6 μm.

In addition to the transmission measurements, we also observed the surface damage and compared the surface characteristics of graphene

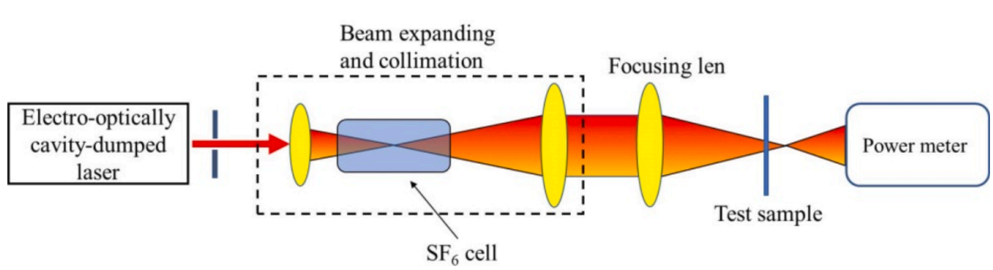

Fig. 1a. Diagram of the experimental platform.

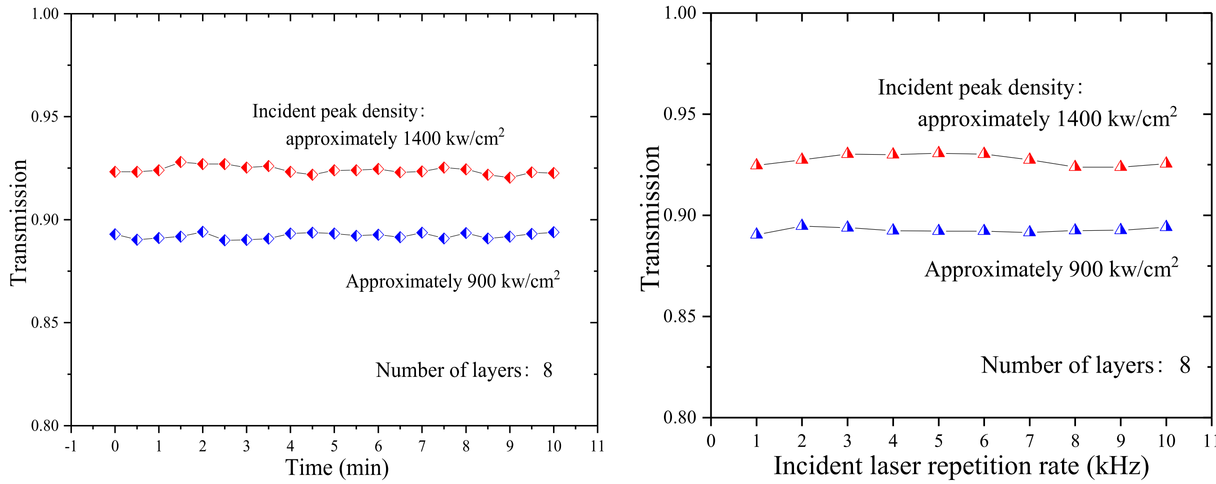

Fig. 3. Stability measurements of graphene transmittance.

before and after the damage occurred. As shown in Fig. 4, the tested graphene film had 8 layers, and there were many white lines on the surface. See Table.2 for the corresponding numbers of the damaged areas shown in Fig. 4. The peak power density of the first irradiation was 1400 kW/cm^2, and the damage traces are shown in area No. 2. When the same power density was used for irradiation, the traces did not change further (and the transmittance did not change). When the incident peak power density was increased, such as in areas No. 1, 3 and 5, the white marks were more obvious and the transmittance was higher. This means that the surface layer of graphene had been ablated and damaged, and the damage threshold was related only to the peak power density.

According to the analysis of the above experimental results, if the number of layers and incident peak power density are fixed, then the transmittance of graphene is highly stable, and the damage threshold of single-layer graphene is above 4 MW/cm^2 at 10.6 μm.

4. Saturable absorption parameters

To extract the saturable absorption parameters of graphene films at 10.6 μm, the measured transmission for films consisting of 1, 4 and 8 layers of graphene were fitted. The fitting results in the range from 0 to 1000 kW/cm^2 are shown in Fig. 5 and Table.3. ΔT is the difference in transmittance between 0 and 1000 kW/cm^2.

The absorption formula of graphene was fitted:

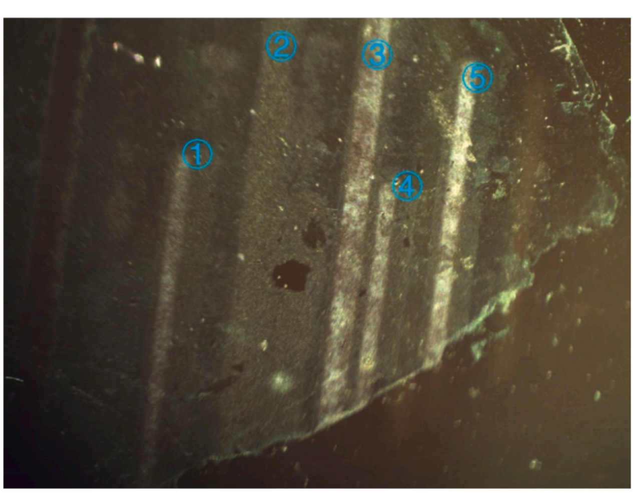

Fig. 4. Graphene surface ablation.

Table 2
Damage areas.

Corresponding numbers in Fig. 4	Peak power (first irradiation) (kW/cm^2)	Peak power (second irradiation) (kW/cm^2)
No.1	1400	1900
No.2	1400	1400
No.3	1400	2600
No.4	1400	2600
No.5	1400	4200

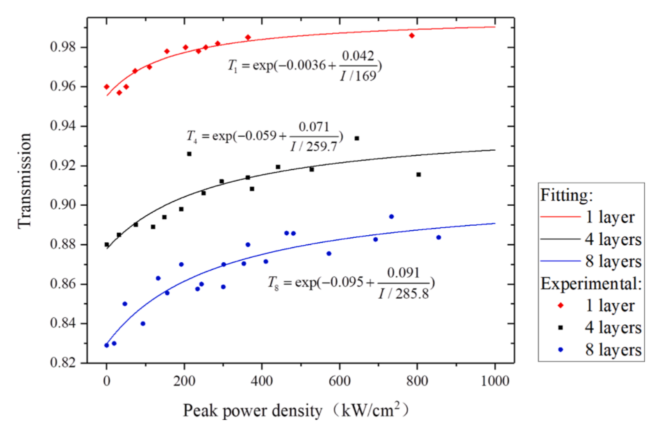

Fig. 5. Graphene transmittance experimental results and fitting.

Table 3
Absorption parameters of graphene films.

Layers	8	4	1
α_{ns} (cm^{-1})	0.095	0.059	0.0036
α_s (cm^{-1})	0.091	0.071	0.042
I_s (kW/cm^2)	285.8	259.7	169
ΔT (%)	6.1	5	3.1

$$T = \exp\left(\alpha_{ns} + \frac{\alpha_s}{I/I_s}\right) \quad (1)$$

The fitting absorption parameters are shown in Table. 3.

An optical isolator must have high isolation and low insertion loss performance. As shown in Table. 3, increasing the number of layers increased the difference of transmittance ΔT, but at the same time, α_s and α_{ns} were directly proportional to the number of layers. That is, the more layers there are, the greater the nonsaturable loss coefficient and initial absorption coefficient. With the increase in the number of layers, the ratio of α_{ns} and α_s also increased. The ratio α_{ns}/α_s first exceeded 1 when the film contained 8 layers, and α_{ns}/α_s was approximately 2 for films that contained 12 layers [11]. The results show that the nonsaturable loss did not increase linearly, but it increased rapidly with increasing number of layers. The values of I_s were 169, 260, 286 and 333 kW/cm^2 for films that contained 1, 4, 8 and 12 layers, respectively. It seems that the saturated light intensity grew more slowly in the presence of more layers.

According to the fitting results for saturable absorption parameters versus the number of layers, the difference in transmittance ΔT increased, which was conducive to the increased isolation capacity of the isolator but also increased the unsaturated loss and insertion loss of the isolator. In addition, the damage threshold of single-layer graphene was higher than that of multilayer graphene. Therefore, the multilayer graphene isolator is suitable for low peak power, and multi-pass single-layer graphene is needed at high power densities.

5. 10.6 μm graphene isolator

According to the above experimental analysis, the graphene film has nonlinear absorption capacity at 10.6 μm, and the small signal absorption coefficient is related only to the number of layers. To improve the isolation ability of the isolator, the number of layers should be increased. However, as shown in the above analysis, the damage resistance of multilayer films is low, and the ratio of the nonsaturable loss coefficient is high, so multi-pass single-layer graphene is suitable for high power densities. The single-layer film has high damage resistance and a low ratio of nonsaturable loss coefficients; thus, it has potential to be used as a 10.6 μm optical isolator. Fig. 6 shows two kinds of single-layer graphene optical isolators. Fig. 6(a) shows a single-layer graphene array, and Fig. 6(b) shows a multi- reflection graphene optical isolator.

We simulate and analyze the influence of the number of layers and small-signal noise contrast on isolation performance. In this paper, the small-signal contrast is defined as the ratio of the small-signal pulse peak power to the main pulse peak power. The relaxation time of the graphene upper energy level is on the order of picoseconds, and the absorption effect continues for the duration of the pulse, so the temporal pulse waveform does not change significantly for the nanosecond amplification system. We sliced an arbitrary input pulse, $I_{in}(t)$, into M small segments of duration Δt in the time domain. The total sampling time $\tau_{total} = M \times \Delta t$, where Δt is the sampling interval and M is the sampling time (integer). Each segment is treated as a square pulse. The output pulse waveform is calculated by $I_{\text{out}}(t) = T \cdot I_{\text{in}}(t)$. As shown in Fig. 7, the peak power of the main pulse is 3 MW/cm^2 (<ablation threshold), and the pulse width is 15 ns. The small signal pulse is 80 ns before the main pulse, and the pulse width is half of the main pulse width. Fig. 7 shows simulation of the pulse waveform evolution of the incident small signal contrast of 1% after 50 passes with single-layer graphene. After 50 passes with single-layer graphene, the small signal contrast was 0.15%, the small signal transmission rate was approximately 10%, and the main pulse transmission rate was approximately 65%. The transmittance difference ΔT was approximately 55%, and the small signal noise light was effectively suppressed.

Fig. 8 shows the variation of the transmittance with the number of passes at 1% and 10% small signal pulse contrast. The transmittance of the main pulse decreased slowly, while the transmittance of the small signal contrast of 1% decreased most rapidly, which proved that the absorption of the small signal was much higher than that of the main pulse. Thus, when the small power signal is smaller, the suppression is stronger.

6. Conclusions

Graphene has great potential as a saturable optical isolator. To study the performance of graphene in a 10.6 μm optical isolator, we built an experimental platform to measure its saturable absorption parameters.

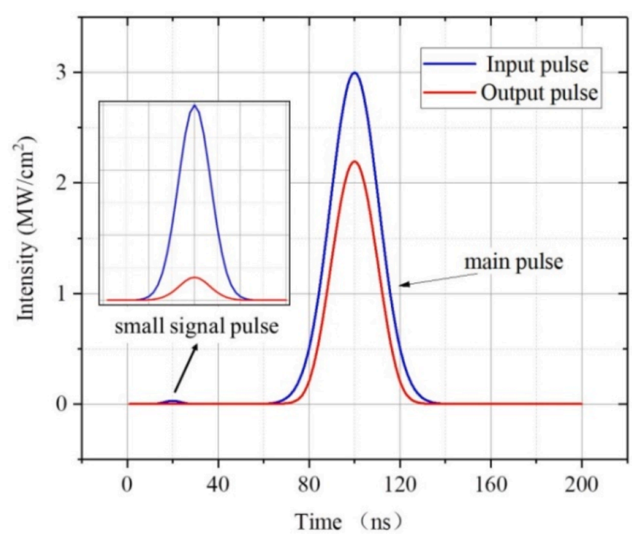

Fig. 7. Pulse waveform evolution of a single graphene film with 50 passes.

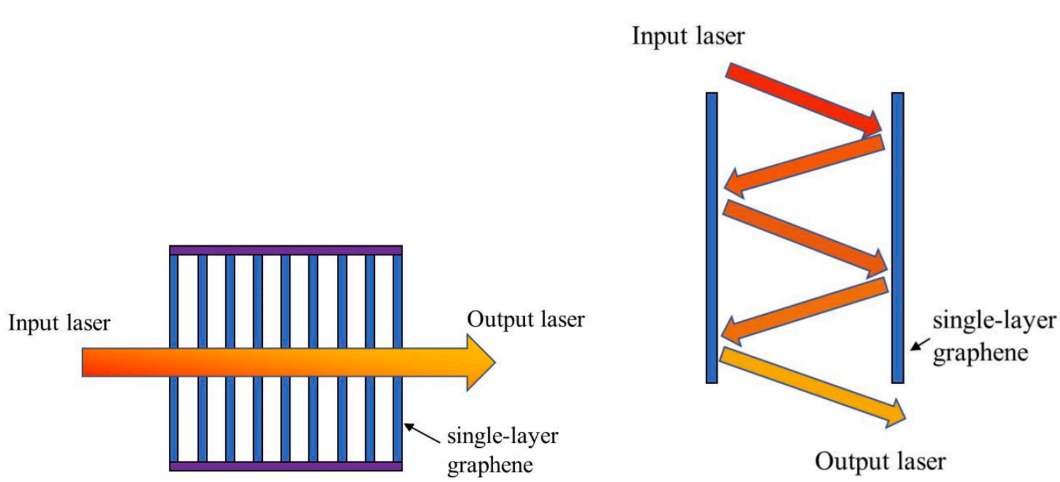

Fig. 6. Transmission and reflection graphene isolators.

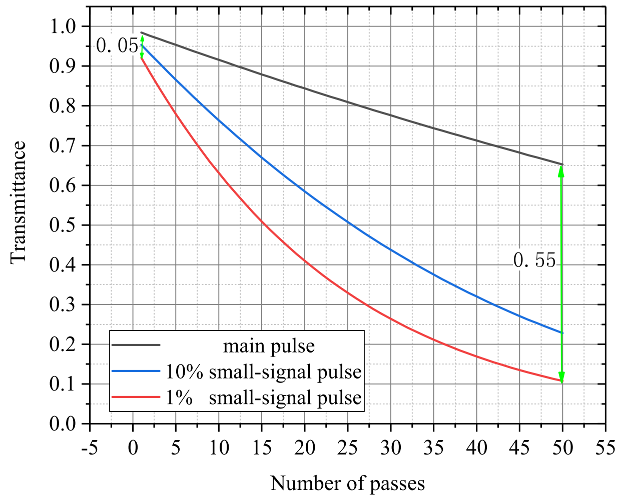

Fig. 8. Transmittance versus number of passes through single graphene.

The experimental results show that the saturable absorption parameters α_s, α_{ns} and I_s are inversely proportional to the number of layers, and the damage threshold is negatively correlated with the number of layers. The single-layer graphene-based ZnSe substrate has excellent saturable absorption characteristics and ablation resistance. We simulated the relationship between the transmission and pulse waveform evolution characteristics and the number of passes through single-layer graphene. The simulation results show that small signal noise light can be effectively suppressed by passing multiple times through single-layer graphene.

Declaration of Competing Interest

The authors declare that they have no known competing financial interests or personal relationships that could have appeared to influence the work reported in this paper.

Acknowledgements

This work was supported by the National Key R&D Program of China NO.2018YFE0203202; State Key Laboratory of Laser Interaction with Matter Project (SKLLIM1914, SKLLIM2114); Science and technology cooperation project between Jilin Province and Chinese Academy of Sciences (2021SYHZ0028);Youth Innovation Promotion Association CAS (2021216); National Natural Science Foundation of China (62104223, 61904178).

References

[1] L. Hilico, A. Douillet, J.P. Karr, E. Tournieì, Note: A high transmission Faraday optical isolator in the 9.2 μm range, Rev. Sci. Instrum. 82 (2011) 553.
[2] K. Nowak, T. Ohta, T. Suganuma, J. Fujimoto, H. Mizoguchi, A. Sumitani, A. Endo, CO_2 laser drives extreme ultraviolet nano-lithography — second life of mature laser technology, Opto-Electron. Rev. 21 (4) (2013), https://doi.org/10.2478/s11772-013-0109-3.
[3] I. Kitazima, H. Iwasawa, Slow Relaxation Processes in SF6 Gas After Pumping by a CO_2 Laser Pulse, Laser Chem. 11 (1) (1991) 39–48.
[4] A.K. Geim, K.S. Novoselov, The rise of graphene, Nat. Mater. 6 (2009) 11–19.
[5] A. Kuzmenko, E. Van Heumen, F. Carbone, d. M. Van, D.,, Universal Optical Conductance of Graphite, Phys. Rev. Lett. 100 (2008), 117401.
[6] J.M. Dawlaty, S. Shivaraman, M. Chandrashekhar, M.G. Spencer, F. Rana, Measurement of Ultrafast Carrier Dynamics in Epitaxial Graphene, MRS Proc. 1081 (2008), https://doi.org/10.1557/PROC-1081-P06-04.
[7] Z. Wang, H. Mu, C. Zhao, Q. Bao, H. Zhang, Harmonic mode-locking and wavelength-tunable Q-switching operation in the graphene–Bi2Te3 heterostructure saturable absorber-based fiber laser, Opt. Eng. 55 (2016), 081314.
[8] H. Wan, W. Cai, F. Wang, S. Jiang, S. Xu, J. Liu, High-quality monolayer graphene for bulk laser mode-locking near 2μm, Opt. Quantum Electron. 48 (2016) 11.
[9] F. Canbaz, N. Kakenov, C. Kocabas, U. Demırbas, A. Sennaroglu, Generation of sub-20-fs pulses from a graphene mode-locked laser, Opt. Express 25 (3) (2017) 2834, https://doi.org/10.1364/OE.25.002834.
[10] A. Pushkin, E. Migal, S. Tokita, Y. Korostelin, F. Potemkin, Femtosecond graphene mode-locked Fe:ZnSe laser at 4.4 um, Opt. Lett. 45 (2020).
[11] V.R. Sorochenko, E.D. Obraztsova, P.S. Rusakov, M.G. Rybin, Nonlinear transmission of CO2 laser radiation by graphene, Quantum Electron. 42 (2012) 907–912.
[12] W.D. Tan, C.Y. Su, R.J. Knize, G.Q. Xie, L.J. Li, D.Y. Tang, Mode locking of ceramic Nd:yttrium aluminum garnet with graphene as a saturable absorber, Appl. Phys. Lett. 96 (2010) 1308.
[13] R.R. Nair, P. Blake, A.N. Grigorenko, K.S. Novoselov, T.J. Booth, T. Stauber, N. Peres, A.K. Geim, Fine Structure Constant Defines Visual Transparency of Graphene, Science 320 (2008).